



Intensify chemical reduction to remove nitrate from groundwater via internal microelectrolysis existing in nano-zero valent iron/granular activated carbon composite

Sihai Hu^{a,b}, Chengjun Zhang^{a,b}, Hairui Yao^{a,b,*}, Cong Lu^{a,b}, Yaoguo Wu^{a,b,*}

^aKey Laboratory of Space Applied Physics and Chemistry, Ministry of Education, Department of Chemistry, School of Science, Northwestern Polytechnical University, Xi'an 710072, P.R. China, Tel./Fax: +86 29 88431672; emails: hsh18621@163.com (S. Hu), 1156035415@qq.com (C. Zhang), herryyao@mail.nwpu.edu.cn (H. Yao), lucong@nwpu@hotmail.com (C. Lu), wuygal@163.com (Y. Wu)

^bSchool of Science, Northwestern Polytechnical University, Youyi Road 127[#], Xi'an 710072, P.R. China

Received 12 December 2014; Accepted 10 June 2015

ABSTRACT

A composite combination of nano-zero valent iron (nZVI) and granular activated carbon (GAC) was introduced to achieve nitrate transformation into nitrogen with minimum byproducts via chemical reduction. The results showed that nitrate removal was significantly intensified and GAC was an excellent partner of nZVI chemical reduction. Both the dispersion and long-term reactivity of nZVI were improved, and more than 80% of nitrate was removed at 10 g/L nZVI/GAC composite within 90 min in steady state. The byproducts of nitrite and ammonium formed in reduction process were below 0.008 and 0.04 mg/L, respectively, and nitrogen was the main end product, which was confirmed by X-ray photoelectron spectroscopy analysis. Moreover, the kinetic model of nitrate reduction by nZVI/GAC composite can be described well by pseudo-first-order reaction kinetic ($R^2 = 0.984$). The intensification is closely related to the dispersion effect of GAC matrix to nZVI and the promotion effect to electrons transfer between nZVI and nitrate pollutant of internal iron-carbon microelectrolysis existing in such a composite. Therefore, the findings are very beneficial to develop an efficient and low-cost chemical remediation method for nitrate-contaminated groundwater.

Keywords: Nitrate; Chemical reduction; nZVI/GAC composite; Iron-carbon microelectrolysis; End products; Groundwater

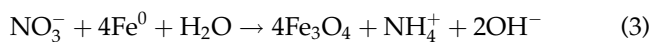
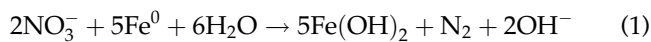
1. Introduction

Groundwater, taken the world over, is an essential and vital resource for most of the countries and extensively used for municipal, domestic, and industrial water supplies [1,2]. In China, 70 percentage of the

population rely on groundwater for their drinking water source [3]. Therefore, groundwater plays a leading role in assuring drinking water safety. However, groundwater is faced with an unprecedented risk of pollution due to an increasing release of various organic and inorganic substances from industrial, agricultural, and domestic activities [4–6]. Remediation of contaminated groundwater is of highest priority since

*Corresponding authors.

the drinking purpose of groundwater. In particular, nitrate, which causes “blue baby syndrome,” is one of the main concerns in groundwater treatment [4,6]. Many technologies including ion exchange, reverse osmosis, distillation, chemical reduction, electrodialysis, and biological denitrification have been used to remove nitrate from groundwater [2,6,7]. Among these methods, chemical reduction is an efficient and economical removal technique [7]. In various chemical reducing agents proposed for nitrate removal, zero valent iron (ZVI) has gained strong interest as an excellent alternative reducing agent. The nitrate reduction reaction by ZVI follows the equations [8]:



Nano-zero valent iron (nZVI, Fe^0) has been reported as an ideal candidate for nitrate-contaminated groundwater remediation because nZVI has shown several advantages such as high reactivity and low dosage compared to conventional ZVI [9]. Furthermore, nZVI is easy to implement *in situ* groundwater treatment by injection or permeable reactive barriers (PRBs) [10,11]. Hence, nitrate elimination by nZVI chemical reduction either *ex-situ* or *in situ* has been received much attention in groundwater treatment [12]. Nevertheless, studies conducted to remove nitrate by nZVI reduction in practical applications show some obstacles as well. First, the final product is liable to ammonium (Eqs. (3) and (4)), which is an undesirable end product [13,14]; second, nZVI tends to form aggregates leading to its surface area and oxidation–reduction potential decrease [8,15]. Thus, ammonium generation and poor stability of nZVI are the main problems that limit its further application in nitrate removal from contaminated groundwater. Therefore, nZVI modification is necessary to realize complete chemical reduction in actual application.

A lot of methods have been reported to enhance nZVI reduction activity and minimize ammonium occurrence [13–15]. Cooperation nZVI with other activity substances such as rare metals, manganese oxides, and activated carbon (AC) is an easily operational method revealed by many researches [16–18]. The research of Comba et al. [14] showed that nitrate and byproduct ammonium could be eliminated by sequential reactions with micrometric ZVI and natural porous

chabasite. Similarly, to reduce the pronounced agglomeration tendency of nZVI, various immobilization techniques are being developed for nZVI stabilization [19]. Bleyl et al. [20] obtained composite hydrophobic particles with good dispersion and high sorption capacity through combination iron and activated carbon colloids (ACC), and the composite material was improved in surface properties and source affinity compared to pure nZVI, which made it particularly suitable for *in situ* remediation of groundwater. Obviously, AC as a porous support is effective in increasing nZVI dispersion, avoiding their agglomeration and decreasing ammonium release.

Recently, iron–carbon internal microelectrolysis reaction has been investigated in pesticide, pharmacy, and dye wastewater treatment [21,22]. Microelectrolysis is based on the reaction of galvanic cell in which electrons are given by galvanic corrosion of microscale sacrificial anodes [23]. Microscopic galvanic cells are formed between iron particles and carbon when a mixture of metal iron with AC in wastewater [24]. Thus, based on such a reaction, numerous microscopic galvanic couples will be spontaneously formed between nZVI and carbon if they are combined together. As a result, electrons transfer between iron and contaminants will be accelerated. Fu et al. [25] found that Reactive Red 195 had much higher degradation efficiency when ZVI and AC combination than single step. Wu et al. [26] studied nZVI-loaded on AC to remove Cr(VI), and their results revealed that Cr(VI) reduction rate was 10 times higher than traditional reaction because C- Fe^0 formed microelectrolysis system which enhanced reaction rate.

However, the galvanic corrosion process of nZVI and AC as a composite for nitrate removal is not investigated up to date, and AC is often used in the form of granular activated carbon (GAC) which is the most widely used adsorbent in wastewater treatment. Consequently, GAC is preferred because of its high sorption ability to inorganic pollutants and excellent surface properties for adjusting nZVI into desired directions. GAC carrier has the potential for increasing pollutant nitrate concentration in the vicinity of active iron surface, and its pores can offer opportunities for finely dispersed nanoiron clusters immobilization. More importantly, internal microelectrolysis formed spontaneously in such a combination system may accelerate electrons transfer where GAC as a medium to promote nitrate reduction. Based on the characteristics of iron–carbon system, via combination nZVI and GAC, nZVI agglomeration and stability would be improved and nitrate removal would be intensified to minimize ammonium and nitrite byproducts as well. Additionally, GAC is benign, easily available and

inexpensive. Hence, in the present study, nZVI and GAC were coupled as a composite (nZVI/GAC) to achieve a complete chemical reduction for nitrate removal from groundwater.

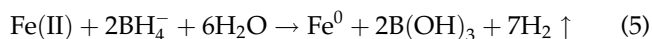
2. Materials and methods

2.1. Materials

Nut shell-derived GAC obtained from Gongyi Tongxin Water Treatment Material Co., Ltd (China) was used as the carrier of nZVI, and the particle size of GAC was 50 mesh (<0.3 mm). To avoid carbon black and other impurities influence, GAC was washed by deionized water ($R > 18 \text{ M}\Omega$) for 4 h and soaked in 1 M HNO_3 for 24 h followed by repeated rinsing with deionized water, and then placed in a vacuum drying oven at 105°C until dry. Actual groundwater was sampled from Xi'an, China, and the detailed sampling and water quality parameters are described in our previously published article [27]. Contaminated groundwater was simulated using actual groundwater consisting of a certain concentration of KNO_3 . All chemical stock solutions were prepared by analytical reagents using deionized water and stored at 4°C unless otherwise specified.

2.2. Preparation of nZVI/GAC composite

The nZVI/GAC composite was prepared with reference to Wang et al. [28] and Kim et al. [29], and some improvements were made in the preparation. In typical synthesis, 1 g of $\text{FeSO}_4 \cdot 7\text{H}_2\text{O}$ and 5 g of GAC were mixed in 200 mL of degassed deionized water. The solution pH was adjusted to 4.0 with 1 M HNO_3 . The mixture was treated with ultrasound for 15 min and then stirred vigorously at ambient temperature for over 12 h to achieve GAC-saturated adsorption of Fe(II) . The slurry was diluted five times using a mixture of ethanol and deionized water (1:1 *v/v*). To ensure efficient reduction of Fe(II) , 25 mL of 1 M NaBH_4 solution was added at 30 drops/min and stirring condition. The reduction reaction is as follows:



After incubation, the black solids were separated from the solution using a vacuum filtration flask (0.45 μm membrane filter) and washed several times with degassed deionized water to remove residual sulfate. Then, the black solids were vacuum dried at 60°C and stored in a N_2 -purged desiccator [30]. Unsupported nZVI particles were also prepared in a similar way

without GAC, and in all synthesis, N_2 was bubbled into solution during the entire process to maintain an inert atmosphere. Iron content in nZVI/GAC composite was determined according to the procedure mentioned in literature [31] and the result was $64.3 \mu\text{mol/g}$.

2.3. Batch experiments

The reduction activity of nZVI/GAC composite was investigated through batch experiments according to description in [8] and [15]. Briefly, the experiments were carried out in a 1-L brown glass bottle (to avoid photolysis) with Teflon rubber plug at atmospheric pressure. The model contaminated groundwater of 500 mL with 50 mg/L of nitrate (NO_3^- -N) and 5 g nZVI/GAC composite were added to the bottles. Before the experiments, to build a low-dissolved oxygen circumstance of groundwater, model groundwater was purged with argon gas for 20 min to strip out dissolved and adsorbed oxygen (oxidation–reduction potential was 203 mv). And the initial pHs of model solutions were adjusted with 0.10 M HCl or NaOH solution. Then the bottles were shaken on a thermostatic reciprocal shaker (Shanghai Yiheng Instruments Co., Ltd, China) with a speed of 50 rpm at $25 \pm 1^\circ\text{C}$. The samples were taken by a syringe at predetermined time intervals and filtered through a $0.45 \mu\text{m}$ syringe filter, and then tested for nitrate, nitrite (NO_2^- -N) and ammonium (NH_4^+ -N) content. To determine the pathway and mechanism of nitrate reduction by nZVI/GAC composite, the transformation products in reduction process were monitored regularly. The nZVI/GAC composite after chemical reduction was characterized as well. The bulk solution in bottles was discarded at a designated reaction time, and the composite that remained in the bottles was washed three times with deionized water and then dried in vacuum drying oven for further characterization. All the prepared samples were taken for analysis immediately. The reduction experiments were conducted in triplicate and analysis showed the relative errors were lower than $\pm 5\%$.

2.4. Analysis methods

The morphology and surface characteristics of nZVI/GAC composite were tested by scanning electron microscopy (SEM; VEGA 3 LMH, TESCAN, Czech) and energy-dispersive X-ray spectra (EDS) were obtained using Oxford INCA X-ACT equipment in SEM. The valence characteristics of iron element in nZVI/GAC composite were determined using X-ray

photoelectron spectroscopy (XPS; Axis Ultra DLD, Kratos, UK) with Al K_{α} radiation. Core level spectra for C 1s, O 1s, N 1s, and Fe 2p were taken at high resolution and analyzed for chemical state information. X-ray diffraction patterns (XRD) spectra were recorded in the range of $2\theta = 10^{\circ}$ – 80° by powder diffractometer (Model D8, Bruker, Germany) with Cu $K_{\alpha 1}$ radiation ($k = 0.154$ nm). The instrument was operated with 40 kV and 30 mA at a scanning speed of $2^{\circ}/\text{min}$ (2θ).

Batch test samples were periodically collected to analyze the concentration of nitrate, nitrite, and ammonium. Standard methods GB5750–2006 in China were adopted for all parameters analysis. Nitrate and nitrite contents were determined by ion chromatography (IC) (792Basic IC, Metrohm, Switzerland) equipped with a separating column (A Supp 5 (6.1006.530), 250 mm \times 4.0 mm) and electrical conductivity detector with NaHCO_3 (1.0 mmol/L)/ Na_2CO_3 (3.2 mmol/L)/methanol (3%) eluent and a total flow rate of 0.6 mL/min. The samples were filtered through 0.45 μm filters and then 20 μl were injected manually through an injection port. The suppressed conductivity detector was maintained at $25 \pm 0.5^{\circ}\text{C}$. The concentration of ammonium released during nitrate reduction was determined by the Nessler's reagent spectrophotometric method. Dissolved iron concentration in solution was analyzed by atomic absorption spectroscopy (AAS) (TAS-990, PERSEE Beijing, China), and pH values were determined by precise pH meter (PHSJ-5, INESA Scientific Instrument Co., Ltd, China).

3. Results and discussion

3.1. Characterization of nZVI/GAC composite

Studies have shown that GAC has abundant pores and functional groups, which provide a good possibility for nZVI particles to be trapped inside of them [21,32,33]. Fig. 1(a) implied that, in the absence of GAC, iron particles were found to rapidly link to chain due to larger surface energy of nanoparticles. Conversely, in Fig. 1(b), the iron particles were well dispersed on surface of GAC carrier without any aggregation and the average particles size were 40–100 nm by comparison with a standard ruler. Hence, SEM images (Fig. 1(a) and (b)) confirm the presence of both iron and GAC in the composite and reveal that iron particles are able to distribute over GAC with nanoscale, and GAC carrier has distinctive dispersion ability to nanoparticles.

Fig. 1(c) is the XRD pattern of nZVI/GAC composite. From Fig. 1(c), it is obvious that the characteristic peaks are at $2\theta = 24.8^{\circ}$, 38.5° , and 44.9° . The broad peak at $2\theta = 24.8^{\circ}$ confirms the presence of GAC in the

composite [17,34]. The diffraction peak at 44.9° observed in the composite samples confirms that iron is zero valence (shown in Fig. 1(c)) as the XRD characteristic peak of zero valent iron is about 45° (2θ) that has been evidenced by some investigations [18,35]. However, the peak at 38.5° can be oxides of iron such as FeO illustrating that nZVI in the composite is core-shell structure and the shell is oxide layer. The crystalline size of nZVI was calculated using the Debye-Scherrer formula and found to be about 50 nm, which was similar to SEM analysis. Moreover, in the XRD spectrum, strong diffraction peaks of Fe_3O_4 ($2\theta = 35.46^{\circ}$, 43.12° , 53.50° , 56.98° , and 62.64°) were not found suggesting that nZVI oxidation did not occur severely after supported on GAC, and thus, it is easy to infer that the nZVI/GAC composite has some antioxidant capacity.

XPS analysis was conducted to observe the chemical states of iron presented on GAC (Fig. 1(d)) and a narrow scan from 740.0 to 700.0 eV was recorded (Fig. 1(e)) as well. From the XPS spectra, significant differences were observed for GAC and nZVI/GAC composite. The peaks at 706.8 and 720.0 eV correspond to Fe $2p_{3/2}$ and Fe $2p_{1/2}$ signals from Fe (0) and the peaks at 710.0 and 725.0 eV binding energy correspond to Fe $2p_{3/2}$ signals from oxidized iron [29,36]. Clearly, the characteristic binding energies at 706.8 and 720.0 eV for Fe $2p_{3/2}$ and Fe $2p_{1/2}$ peaks confirm Fe (0) existence. The two intense peaks observed at 710.0 and 725.0 eV indicate that iron oxides (FeO or Fe_2O_3) are also existent on the surface of nZVI in the composite, which is consistent with previously published studies [29,35,36]. Therefore, the multiple iron valence states presence demonstrate iron nanoparticles supported on GAC matrix have a core-shell structure with a core of zero valent iron (Fe^0) and a shell of iron oxide or hydroxide. As described in the literature [28,29], the overlayer is thought to form spontaneously during synthesis and handling of the composite in an aqueous solution. These findings are in good agreement with those obtained from SEM and XRD analysis, which suggests nZVI particles disperse on GAC carrier as well. The content of nZVI in the composite was determined by EDS and the result is exhibited in Fig. 1(f). Iron content is high to 64.51% in the surface of nZVI/GAC composite suggesting that nZVI has been supported on GAC successfully and Fe^0 is the main constituent of the composite. Overall, Fig. 1 illustrates that nZVI particles uniformly disperse on the surface of GAC matrix with a core-shell structure and average diameter of 40–100 nm. Obviously, the dispersion of nZVI was significantly improved and nZVI content reaches to 64.51% in the surface of nZVI/GAC composite, which is favorable for nitrate complete reduction.

3.2. Intensity removal of nitrate from groundwater by nZVI/GAC composite

For comparison, the additional dosage of bare nZVI or GAC was equal to the amount of nZVI or GAC calculated by nZVI-loaded amount in the composite. The results of nitrate removal by nZVI, GAC, and nZVI/GAC composite are depicted in Fig. 2(a). As shown in the traces, nitrate removal rates were measured to be 35.9% for nZVI, 41.5% for GAC, and 81.1% for nZVI/GAC composite after reaction 90 min, respectively. These results show that GAC has absorption capability to nitrate due to its abundant pores and functional groups and nZVI has reduction ability leading to nitrate decrease. Nitrate removal rate by the composite is apparently higher than single nZVI or

GAC. Hence, both nZVI and GAC are positive to nitrate removal, but the removal ratios are low because of limited adsorption sites of GAC and too high activity of bare nZVI [37]. Moreover, the removal ratio by nZVI/GAC composite was higher than the sum of single GAC and nZVI. These phenomena strongly illustrate that the process of nitrate removal by nZVI/GAC composite is not only a combination of GAC adsorption and nZVI reduction, but also some synergetic effects exist in such a composite. In addition, the removal by bare nZVI mainly occurred at the beginning of reaction (about 30 min), which was reported by many investigations [9,18], and this feature is unfavorable in the field application such as PRBs. By comparison, Fig. 2(a) explicitly shows that nZVI/GAC

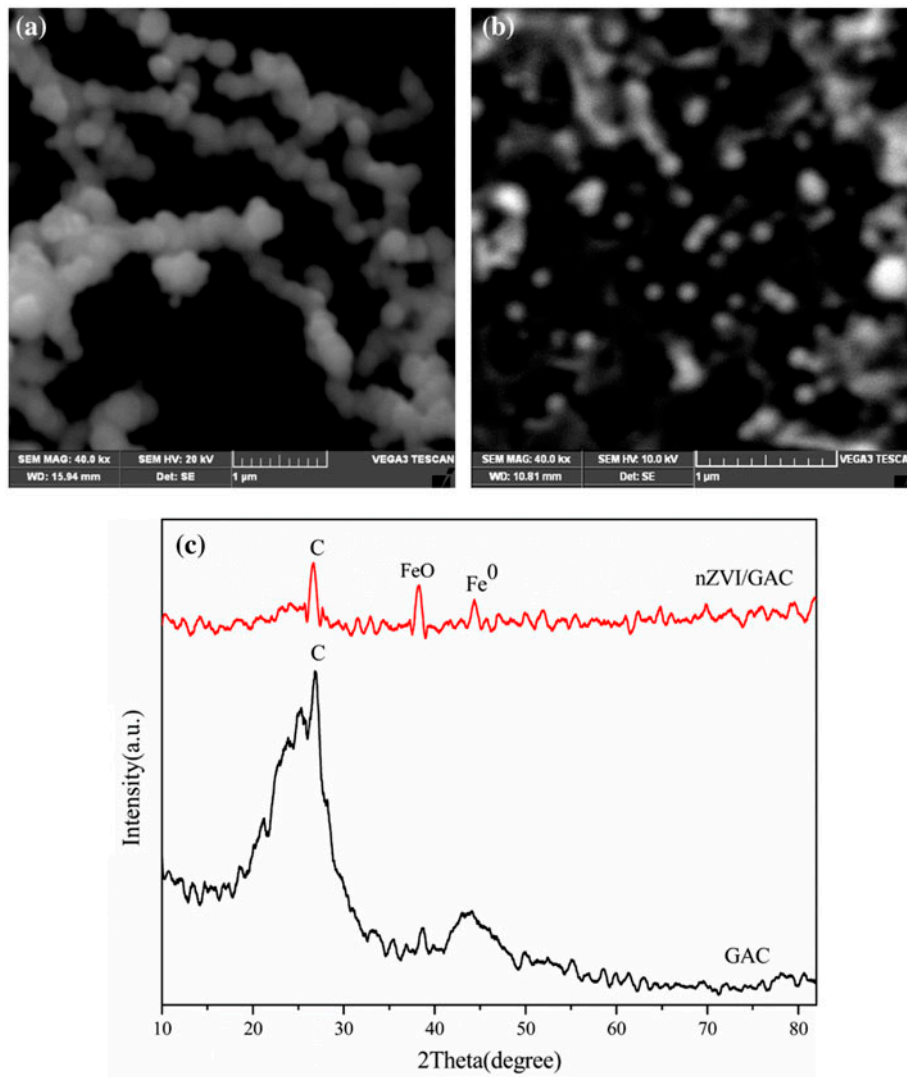


Fig. 1. (a, b) SEM images, (c) XRD pattern, (d, e) XPS, and (f) EDS of the nZVI/GAC composite.

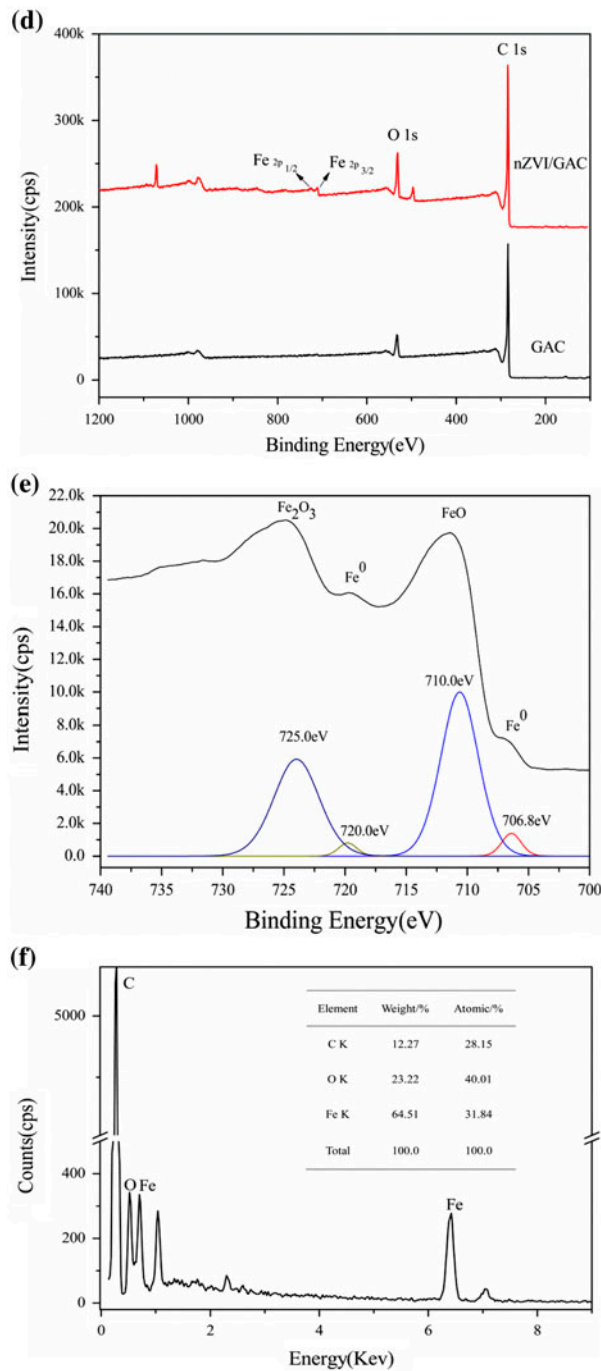


Fig. 1. (Continued).

composite can still remove nitrate after reaction of 60 min under experimental conditions. This suggests that the long-term reactivity of nZVI is significantly improved after supported on GAC, which is a great advantage for nitrate removal in real application.

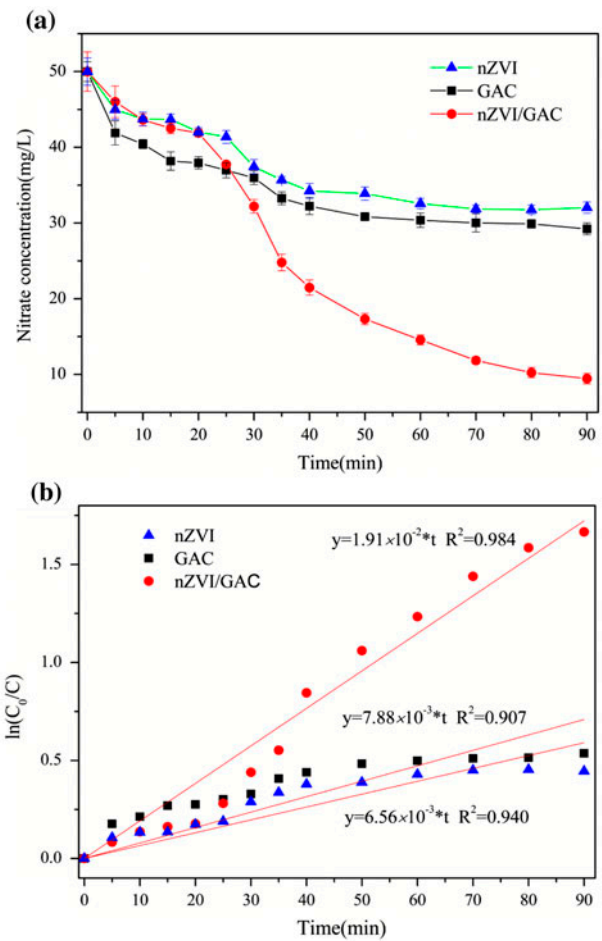


Fig. 2. (a) Nitrate reduction and (b) relationship between $\ln(C_0/C)$ and reaction time. Initial nitrate concentration was 50 mg/L and pH value was adjusted to 7.5.

The removal reaction can be described as a pseudo-first-order reaction with respect to nitrate concentration as given in Eq. (6):

$$v = -d[\text{NO}_3^-]/dt = k_{\text{obs}}[\text{NO}_3^-] \quad (6)$$

where k_{obs} is the observed first-order reaction rate constant, which is the slope of the regression lines obtained by plotting a natural logarithm graph with respect to nitrate concentration and reaction time according to Eq. (7):

$$\ln([\text{NO}_3^-]_0/[\text{NO}_3^-]) = k_{\text{obs}}t \quad (7)$$

where $[\text{NO}_3^-]_0$ is equal to the initial nitrate concentration. The relationship between $\ln([\text{NO}_3^-]_0/[\text{NO}_3^-])$ (\ln

(C_0/C) and the reaction time is presented in Fig. 2(b). A linear regression of the first-order kinetic Eq. (7) is performed for each group of data. The k_{obs} values are 6.56×10^{-3} , 7.88×10^{-3} and $1.91 \times 10^{-2} \text{ min}^{-1}$ for nZVI, GAC, and nZVI/GAC composite, respectively. The k_{obs} prominently increased and difference for nZVI and nZVI/GAC composite means that the kind of reducing agent has significant effect on k_{obs} . Moreover, the fitting of the data for nZVI/GAC composite is fit well to linear model ($R^2 = 0.984$), which provides strong evidence that the removal reaction by the composite is pseudo-first-order reaction. Similar results were observed as well in other studies about the reaction of Fe^0 powder with nitrate [8,34].

3.3. End products of nitrate removal by nZVI/GAC composite

The products of reduction reaction by Fe^0 are consistent with the occurrence of aforementioned reaction Eqs. (1)–(4) reported in the literatures [8,9,14]. From the equations, it can be seen that there are three main products of nitrogen, nitrite, and ammonium in nitrate removal process by nZVI reduction. Accordingly, the reaction path can be determined according to product species because different reactions have different products, in other words, products can be used as indicators of nitrate reduction and are benefit to infer reaction mechanism. However, many previous studies reported that the major product of nitrate reduction in the $\text{Fe}^0\text{-H}_2\text{O}$ system was ammonium or nitrite [13,14], and both of them were unexpected end products in nitrate removal from groundwater. Therefore, nitrite and ammonium concentration were measured at the predetermined time of experiments, and the results are showed in Fig. 3.

As depicted in Fig. 3, nitrite and ammonium generation dramatically decreased in nitrate reduction process by nZVI/GAC composite. For the composite, both the maximum and final concentrations were lower than for nZVI. In particular, an extremely small amount of nitrite and ammonium that below 0.008 and 0.04 mg/L, respectively, were observed after reaction of 90 min, and by this time the concentrations almost reached to the limits of detection (0.003 and 0.025 mg/L). Thus, the results indicate that the participation of GAC in nitrate reduction by nZVI particles can significantly decrease nitrite and ammonium residue. Furthermore, from Fig. 2(a) and Fig. (3), the total amount of residual nitrate, nitrite, and ammonium was lower than initial nitrate concentration (50 mg/L) suggesting that nitrate was transformed to nitrogen.

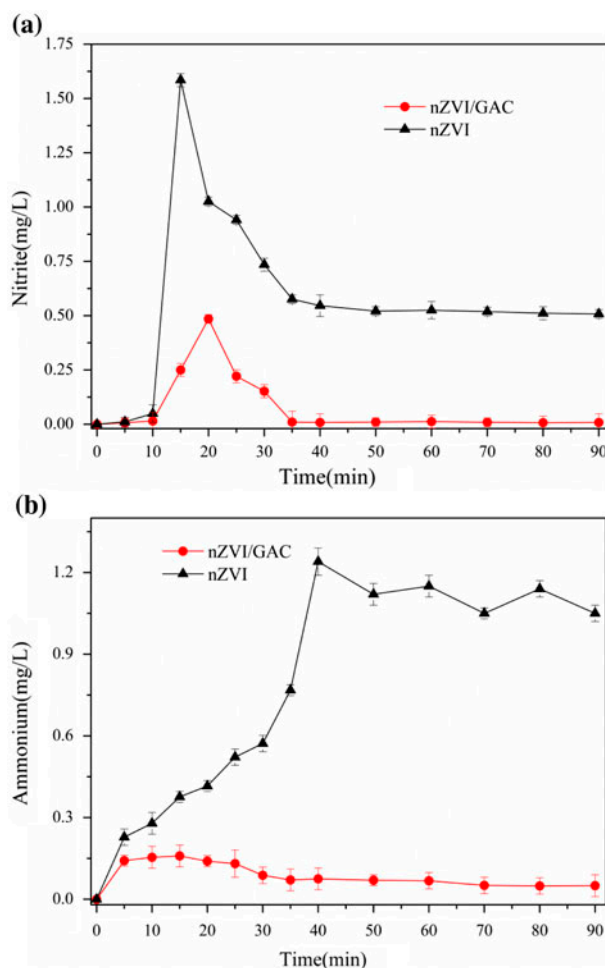


Fig. 3. The change of (a) nitrite and (b) ammonium concentration during nitrate reduction by nZVI/GAC composite.

Therefore, the low level of nitrite and ammonium illustrated that Eq. (1) was the dominant reaction. Nitrogen which was innocuous and could easily escape from water was the dominant end product of nitrate reduction by nZVI/GAC composite under our experimental conditions. The results were similar to the findings of Choe et al. [38] and Hu et al. [39] that nitrate was reduced to nitrogen and almost no intermediates were detected.

3.4. Fate of nZVI/GAC composite during nitrate reduction

The SEM images, XRD patterns, and XPS spectra of nZVI/GAC composite collected after reaction for 90 min were also obtained and presented in Fig. (4). Fig. 4(a) and (b) suggests that the nZVI was oxidized into iron oxides and further precipitation or

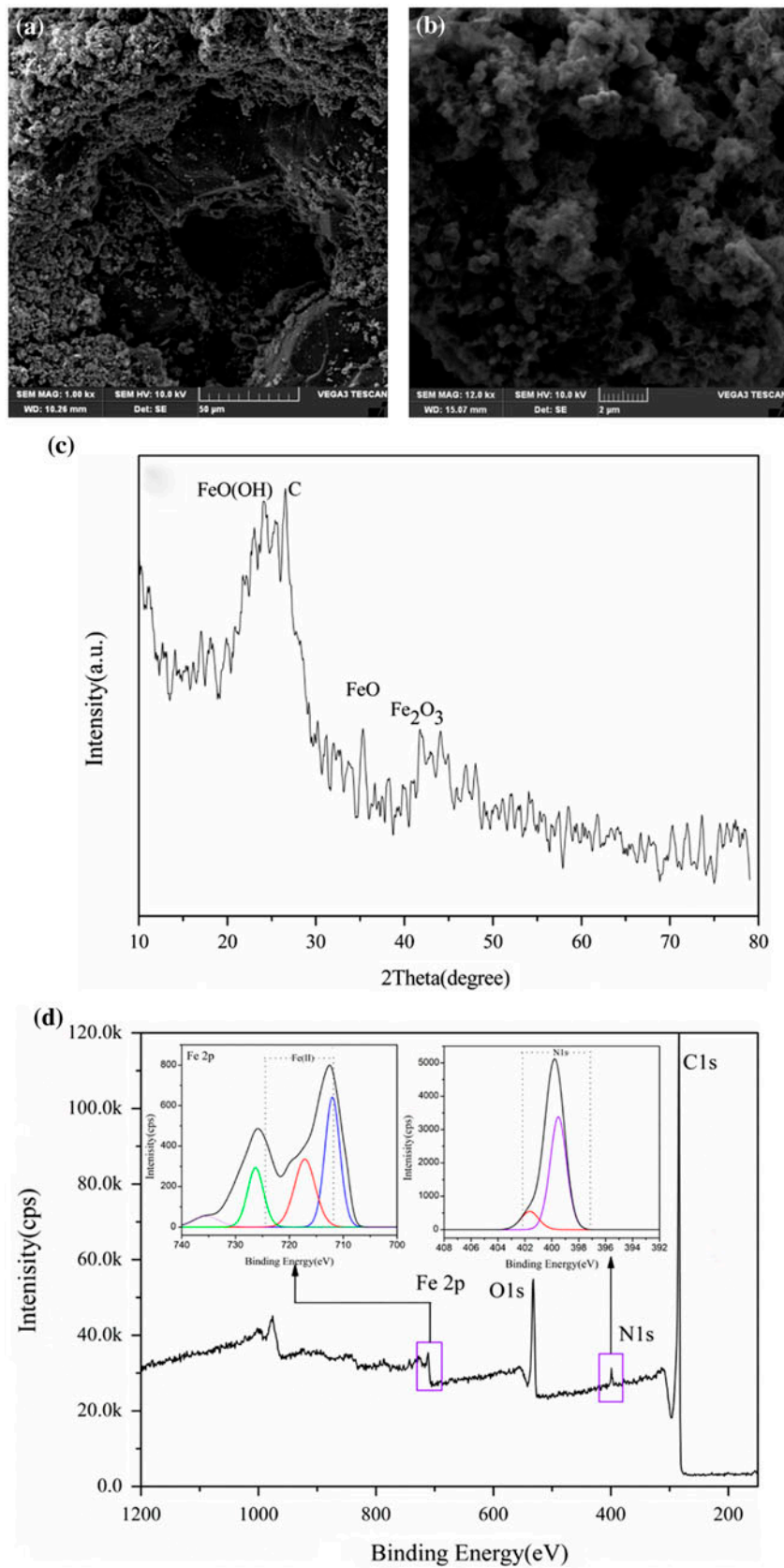


Fig. 4. (a, b) SEM images, (c) XRD pattern, and (d) XPS of nZVI/GAC composite after reaction.

adsorption on GAC matrix. As seen in the XRD patterns (Fig. 4(c)), the characteristic peaks of nZVI changed obviously before (Fig. 1(c)) and after reduction reaction (Fig. 4(c)). After reaction, the XRD peaks of Fe^0 was missing and iron oxides peaks were observed at 24.3° , 35.4° , and 41.7° (2θ), possibly associated with $\text{FeO}(\text{OH})$, FeO , and Fe_2O_3 [40]. Hence, the XRD analysis confirms that nZVI particles are transformed to iron oxides after nitrate reduction, which is consistent with the SEM analysis. The formation of Fe_2O_3 is possible association with iron in water oxidized into iron rust observed by many researches [10,12].

As shown in XPS analysis (Fig. 4(d)), the characteristic peaks of Fe (0) were not observed. The strong photoelectron peaks of Fe $2p_{3/2}$ at around 712.0 and 710.5 can be assigned to Fe(II) and a weak peak Fe $2p_{1/2}$ located at 725.3 eV can be assigned to Fe(III) [31], which reflected the formation of Fe(II) (hydr)oxides as the speculated main products rather than Fe (III). Hence, main end product of nZVI/GAC is iron hydroxide ($\text{Fe}(\text{OH})_2$) with minor hematite (Fe_2O_3), which is in good agreement with XRD results. Thus, the reaction (1) is believed to be more acceptable to explain the intensity effect to complete chemical reduction induced by nZVI/GAC composite. Moreover, the peaks at binding energy between 398.0 and 402.0 eV designates the presence of nitrogenous species as nitrogen because of GAC's adsorption confirmed by Choe et al. [38] and Hu et al. [39]. The results support that nitrate is mainly converted into nitrogen and Eq. (1) overwhelmingly dominates the reaction, which agrees well with the analysis of nitrite and ammonium.

In addition, the iron content in the composite after reduction was confirmed by EDS (Fig. 5(a)). According to the EDS quantification, we found that, before and after reaction, the percentage of oxygen increased from 23.22 (Fig. 1(f)) to 34.94%; meanwhile, the percentage of iron decreased from 64.51 to 51.54%, illustrating that zero valent iron was oxidized as well. However, the iron content was only small change suggesting that iron was still in GAC carrier after reduction because of the absorption of GAC. Consequently, the leaching of dissolved iron after reaction was < 1.0 mg/L as shown in Fig. 5(b). Obviously, only a slight part of dissolved iron ion was detected indeed since most of iron species formation in reduction process might have been encapsulated by GAC matrix. The dissolved iron decreased as spent iron species were concentrated by GAC. As a result, the leaching of iron can be effectively controlled in the participation of GAC, which is believed to be another advantage for utilization of nZVI/GAC composite.

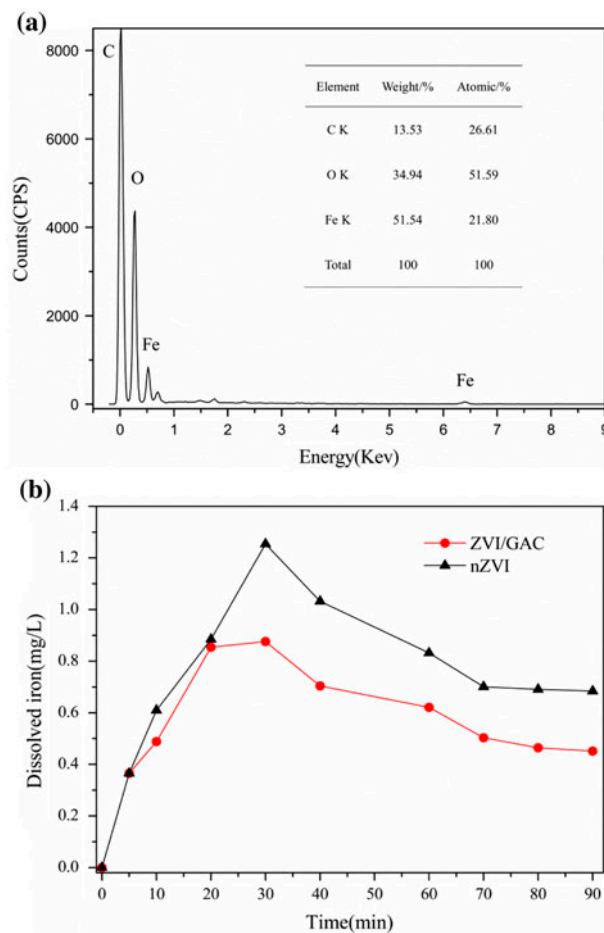


Fig. 5. The (a) EDS of nZVI/GAC and (b) dissolved iron in the solution after reduction reaction.

3.5. Intensity mechanism analysis of nitrate removal by nZVI/GAC composite

Several research papers reported different reaction pathway in the case of adaptation of nZVI compared to conventional ZVI [7,9,41]. The research using nZVI showed that nitrite, nitrogen, and ammonium could be possible products of nitrate reduction. An et al. described that the final product was most ammonium, which was an undesirable end product [13]. However, Hwang et al. suggested that the final reaction product would be nitrogen, which was an ideal product of nitrate reduction [9]. Obviously, a clear pathway and nitrogen species over reaction time have not been determined. Consequently, research on the fate of nitrate and nZVI/GAC should be studied to understand the reaction mechanism during nitrate reduction by nZVI/GAC composite.

Based on the above analysis, little byproducts nitrite and ammonium were detected and the fate of

nZVI in the composite was main Fe(II). In addition to the limited GAC adsorption of nitrite and ammonium, nitrate was mostly converted to nitrogen and accordingly, the primary pathway of nitrate reduction was suggested and shown in Eq. (1) and the intensified mechanism was proposed for nitrate removal by nZVI/GAC composite. First, nZVI particles disperse on GAC very well without agglomeration, so their contact opportunity with pollutant nitrate is increased to improve chemical reduction efficiency. Second, and most important, iron and GAC can spontaneously form a micro-galvanic cell which has been observed in other experiments [18,42–45], and an internal iron–carbon microelectrolysis effect exists in such an nZVI/GAC composite, so electron transfer is greatly accelerated due to GAC as migration medium. Under these factors, nZVI particles in GAC matrix have more opportunities to reduce nitrate to nitrogen. Overall, the composite combined nZVI and GAC is an excellent material for nitrate removal because of no agglomeration and excessive ammonium yield.

4. Conclusions

In this paper, nZVI/GAC composite was prepared and its application to nitrate removal was systematically investigated, with particular emphasis on products and nZVI fate analysis in reduction process. As much as 81.1% nitrate removal rate was obtained within 90 min under the experimental conditions and byproducts nitrite and ammonium formation were <0.008 and 0.04 mg/L, respectively. Moreover, the nitrate reduction by nZVI/GAC composite can be well described by pseudo-first-order reaction kinetic. The nZVI/GAC composite has dual functions of adsorption and chemical reduction, and the involvement of GAC not only intensified nitrate reduction to nitrogen, but also reduced byproducts nitrite and ammonium generation. The intensification can be attributed to two effects: the dispersion effect of GAC to nZVI and the internal iron–carbon microelectrolysis to electron transfer impetus effect. This novel composite represents an important insight on development of new inexpensive and efficient material to groundwater remediation, and of course the mechanism and influence factors need to be thoroughly researched in further studies.

Acknowledgments

The project was financially supported by the National Natural Science Foundation of China (Grant No. 40872164), fund for basic research from the North-

western Polytechnical University (no. JCY20130145), China geological survey project (12120114056201), and graduate starting seed fund of Northwestern Polytechnical University (Z2015147), and the authors gratefully acknowledged them.

References

- [1] D.E. John, J.B. Rose, Review of factors affecting microbial survival in groundwater, *Environ. Sci. Technol.* 39 (2005) 7345–7356.
- [2] A. Bhatnagar, M. Sillanpää, A review of emerging adsorbents for nitrate removal from water, *Chem. Eng. J.* 168 (2011) 493–504.
- [3] M. Samake, Z.H. Tang, W. Hlaing, I.N. Mbue, K. Kasereka, W.O. Balogun, Groundwater vulnerability assessment in shallow aquifer in Linfen Basin, Shanxi Province, China using DRASTIC model, *J. Sustainable Dev.* 4 (2011) 53–71.
- [4] X.T. Ju, C.L. Kou, F.S. Zhang, P. Christie, Nitrogen balance and groundwater nitrate contamination: Comparison among three intensive cropping systems on the North China Plain, *Environ. Pollut.* 143 (2006) 117–125.
- [5] K.R. Burow, B.T. Nolan, M.G. Rupert, N.M. Dubrovsky, Nitrate in groundwater of the United States, 1991–2003, *Environ. Sci. Technol.* 44 (2010) 4988–4997.
- [6] J.H. Qu, M.H. Fan, The current state of water quality and technology development for water pollution control in China, *Crit. Rev. Environ. Sci. Technol.* 40 (2010) 519–560.
- [7] T. Suzuki, M. Moribe, Y. Oyama, M. Niinae, Mechanism of nitrate reduction by zero-valent iron: Equilibrium and kinetics studies, *Chem. Eng. J.* 183 (2012) 271–277.
- [8] H.Y. Liu, M. Guo, Y. Zhang, Nitrate removal by Fe 0/Pd/Cu nano-composite in groundwater, *Environ. Technol.* 35 (2014) 917–924.
- [9] Y.H. Hwang, D.G. Kim, H.S. Shin, Mechanism study of nitrate reduction by nano zero valent iron, *J. Hazard. Mater.* 185 (2011) 1513–1521.
- [10] C.D. Rocca, V. Belgiorno, S. Meriç, Heterotrophic/autotrophic denitrification (HAD) of drinking water: Prospective use for permeable reactive barrier, *Desalination* 210 (2007) 194–204.
- [11] A. Weber, A.S. Ruhl, R.T. Amos, Investigating dominant processes in ZVI permeable reactive barriers using reactive transport modeling, *J. Contam. Hydrol.* 151 (2013) 68–82.
- [12] S.J. Liu, Z.Y. Zhao, J. Li, J. Wang, Y. Qi, An anaerobic two-layer permeable reactive biobarrier for the remediation of nitrate-contaminated groundwater, *Water Res.* 47 (2013) 5977–5985.
- [13] Y. An, T.L. Li, Z.H. Jin, M.Y. Dong, Q.Q. Li, S.M. Wang, Decreasing ammonium generation using hydrogenotrophic bacteria in the process of nitrate reduction by nanoscale zero-valent iron, *Sci. Total Environ.* 407 (2009) 5465–5470.
- [14] S. Comba, M. Martin, D. Marchisio, R. Sethi, E. Barberis, Reduction of nitrate and ammonium adsorption using microscale iron particles and zeolite, *Water Air Soil Pollut.* 223 (2012) 1079–1089.

- [15] H. Park, Y.M. Park, S.K. Oh, K.M. You, S.H. Lee, Enhanced reduction of nitrate by supported nanoscale zero-valent iron prepared in ethanol-water solution, *Environ. Technol.* 30 (2009) 261–267.
- [16] M.A. Oturan, J.J. Aaron, Advanced oxidation processes in water/wastewater treatment: Principles and applications. A review, *Crit. Rev. Env. Sci. Technol.* 44 (2014) 2577–2641.
- [17] L.H. Huang, S.J. Zhou, F. Jin, J. Huang, N. Bao, Characterization and mechanism analysis of activated carbon fiber felt-stabilized nanoscale zero-valent iron for the removal of Cr(VI) from aqueous solution, *Colloid and Surf., A* 447 (2014) 59–66.
- [18] P. Singh, P. Raizada, S. Kumari, A. Kumar, D. Pathania, P. Thakur, Solar-Fenton removal of malachite green with novel Fe0-activated carbon nanocomposite, *Appl. Catal., A: Gen.* 476 (2014) 9–18.
- [19] F.S. Fatemina, C. Falamaki, Zero valent nano-sized iron/clinoptilolite modified with zero valent copper for reductive nitrate removal, *Process Saf. Environ.* 91 (2013) 304–310.
- [20] S. Bleyl, F.D. Kopinke, K. Mackenzie, Carbo-iron[®]—synthesis and stabilization of Fe(0)-doped colloidal activated carbon for *in situ* groundwater treatment, *Chem. Eng. J.* 191 (2012) 588–595.
- [21] M.C. Macías Pérez, C. Salinas Martínez de Lecea, A. Linares Solano, Platinum supported on activated carbon cloths as catalyst for nitrobenzene hydrogenation, *Appl. Catal., A: Gen.* 151 (1997) 461–475.
- [22] J.H. Luo, G.Y. Song, J.Y. Liu, G.R. Qian, Z.P. Xu, Mechanism of enhanced nitrate reduction via micro-electrolysis at the powdered zero-valent iron/activated carbon interface, *J. Colloid Interface Sci.* 435 (2014) 21–25.
- [23] Y. Kato, M. Machida, H. Tatsumoto, Inhibition of nitrobenzene adsorption by water cluster formation at acidic oxygen functional groups on activated carbon, *J. Colloid Interface Sci.* 322 (2008) 394–398.
- [24] Q. Zhang, Treatment of oilfield produced water using Fe/C micro-electrolysis assisted by zero-valent copper and zero-valent aluminium, *Environ. Technol.* 36 (2015) 515–520.
- [25] J. Fu, Z. Xu, Q.S. Li, S. Chen, S.Q. An, Q.F. Zeng, H.L. Zhu, Treatment of simulated wastewater containing Reactive Red 195 by zero-valent iron/activated carbon combined with microwave discharge electrodeless lamp/sodium hypochlorite, *J. Environ. Sci.* 22 (2010) 512–518.
- [26] L.M. Wu, L.B. Liao, G.C. Lv, F.X. Qin, Y.J. He, X.Y. Wang, Micro-electrolysis of Cr (VI) in the nanoscale zero-valent iron loaded activated carbon, *J. Hazard. Mater.* 254–255 (2013) 277–283.
- [27] S.H. Hu, Y.G. Wu, L. Wang, H.Y. Yao, T. Li, Simultaneous removal of nitrate and aniline from groundwater by cooperating heterotrophic denitrification with anaerobic ammonium oxidation, *Desalin. Water Treat.* 52 (2014) 7937–7950.
- [28] W. Wang, M. Zhou, Q. Mao, J. Yue, X. Wang, Novel NaY zeolite-supported nanoscale zero-valent iron as an efficient heterogeneous Fenton catalyst, *Catal. Commun.* 11 (2010) 937–941.
- [29] S.A. Kim, S. Kamala-Kannan, K.J. Lee, Y.J. Park, P.J. Shea, W.H. Lee, H.M. Kim, B.T. Oh, Removal of Pb(II) from aqueous solution by a zeolite-nanoscale zero-valent iron composite, *Chem. Eng. J.* 217 (2013) 54–60.
- [30] Z.M. Gu, J. Fang, B.L. Deng, Preparation and evaluation of GAC-based iron-containing adsorbents for arsenic removal, *Environ. Sci. Technol.* 39 (2005) 3833–3843.
- [31] H.J. Zhu, Y.F. Jia, X. Wu, H. Wang, Removal of arsenic from water by supported nano zero-valent iron on activated carbon, *J. Hazard. Mater.* 172 (2009) 1591–1596.
- [32] V. Subbaramaiah, V.C. Srivastava, I.D. Mall, Catalytic oxidation of nitrobenzene by copper loaded activated carbon, *Sep. Purif. Technol.* 125 (2014) 284–290.
- [33] Y.F. Su, Y.L. Cheng, Y.H. Shih, Removal of trichloroethylene by zerovalent iron/activated carbon derived from agricultural wastes, *J. Environ. Manage.* 129 (2013) 361–366.
- [34] C. Chang, F. Lian, L.Y. Zhu, Simultaneous adsorption and degradation of γ -HCH by nZVI/Cu bimetallic nanoparticles with activated carbon support, *Environ. Pollut.* 159 (2011) 2507–2514.
- [35] Y.L. Zhang, K. Zhang, C.M. Dai, X.F. Zhou, Performance and mechanism of pyrite for nitrobenzene removal in aqueous solution, *Chem. Eng. Sci.* 111 (2014) 135–141.
- [36] X.Q. Li, W.X. Zhang, Sequestration of metal cations with zerovalent iron nanoparticles—A study with high resolution X-ray photoelectron spectroscopy (HR-XPS), *J. Phys. Chem. C* 111 (2007) 6939–6946.
- [37] R. Thankappan, T.V. Nguyen, S.V. Srinivasan, S. Vigneswaran, J. Kandasamy, P. Loganathan, Removal of leather tanning agent syntan from aqueous solution using Fenton oxidation followed by GAC adsorption, *J. Ind. Eng. Chem.* 21 (2015) 483–488.
- [38] S. Choe, Y.Y. Chang, K.Y. Hwang, J. Khim, Kinetics of reductive denitrification by nanoscale zero-valent iron, *Chemosphere* 41 (2000) 1307–1311.
- [39] H.Y. Hu, N. Goto, K. Fujie, Effect of pH on the reduction of nitrite in water by metallic iron, *Water Res.* 35 (2001) 2789–2793.
- [40] J. Yang, Y.L. Guo, D.C. Xu, L.M. Cao, J.P. Jia, A controllable Fe⁰-C permeable reactive barrier for 1, 4-dichlorobenzene dechlorination, *Chem. Eng. J.* 203 (2012) 166–173.
- [41] J.H. Zhang, Z.W. Hao, Z. Zhang, Y.P. Yang, X.H. Xu, Kinetics of nitrate reductive denitrification by nanoscale zero-valent iron, *Process Saf. Environ.* 88 (2010) 439–445.
- [42] Y.Y. Yao, L. Wang, L.J. Sun, S. Zhu, Z.F. Huang, Y.J. Mao, W.Y. Lu, W.X. Chen, Efficient removal of dyes using heterogeneous Fenton catalysts based on activated carbon fibers with enhanced activity, *Chem. Eng. Sci.* 101 (2013) 424–431.
- [43] H.M. Zhou, Y.Y. Shen, P. Lv, J.J. Wang, J. Fan, Degradation of 1-butyl-3-methylimidazolium chloride ionic liquid by ultrasound and zero-valent iron/activated carbon, *Sep. Purif. Technol.* 104 (2013) 208–213.
- [44] X.M. Dou, R. Li, B. Zhao, W.Y. Liang, Arsenate removal from water by zero-valent iron/activated carbon galvanic couples, *J. Hazard. Mater.* 182 (2010) 108–114.
- [45] H.M. Zhou, P. Lv, Y.Y. Shen, J.J. Wang, J. Fan, Identification of degradation products of ionic liquids in an ultrasound assisted zero-valent iron activated carbon micro-electrolysis system and their degradation mechanism, *Water Res.* 47 (2013) 3514–3522.